Science of Sintering, **55** (2023) 171-187

https://doi.org/10.2298/SOS220404007I

UDK: 692.533.1; 691.73; 676.056.73

Production of Ni-Co-Bronze Composites with Different TiC Composition by Hot Pressing

Anil Imak[1], Musa Kilic[2], Ihsan Kirik[3*)]

[1]Bingol University, Faculty of Engineering and Architecture, Department of Mechanical Engineering, Bingol, Turkey

[2]Batman University, Faculty of Technology, Department of Manufacturing Engineering, Batman, Turkey

[3]Bingol University, Vocational High School of Technical Sciences, Department of Machinery, Bingol, Turkey

Abstract:

Improving microstructural, mechanical, and thermal properties of Ni-Co-Bronze composites is crucial for various applications. In this study, five Ni-Co-Bronze (CuSn)+XTiC (0, 3, 7, 10, and 15 wt.%) composites were produced by using the hot pressing method. The effect of TiC reinforcement rate on each of their microstructure, wear, hardness, and thermal properties was investigated. Within the scope of microstructure analysis, the scanning electron microscope (SEM), electron dispersive spectrometer (EDS), and XRD analysis were employed. Thermal analyses were carried out for thermal differences between the samples. Furthermore, microhardness, impact, and wear tests were run to estimate mechanical behaviors of Ni-Co Bronze+XTiC composite. Experimental results indicated that TiC rate had an important effect on the microstructure, wear-resistance and microhardness of Ni-Co bronze composite. As the TiC reinforcement rate increased, the hardness of Ni-Co Bronze+XTiC composites varied between 180 HV and 450 HV. Consequently, microstructure analysis revealed that there was a serious interaction between reinforcement and matrix. Wear resistance increased with a TiC (7-10) wt.% rate but decreased at high TiC rates. It was clearly seen that the wear pattern was both oxidative and abrasive.

Keywords*: Ni-Co Bronze+XTiC composites; Hot pressing; Thermal analysis; Impact toughness; Worn surface analysis.*

1. Introduction

The usage of traditional engineering materials is limited due to their features like weightiness, density, strength, and hardness. However, composite materials have precise distribution of reinforcement rate in the applications. Metal matrix composites (MMC) have physical and mechanical properties in a wide range of engineering applications [1-3]. MMCs are manufactured using various methods such as metal spraying, in-situ composites, powder metallurgy, and hot pressing. Among these methods, powder metallurgy (PM) is particularly common [4,5]. Due to its simplicity, the PM is used commonly to produce composite materials with magnesium alloy matrix [6], aluminum alloy matrix [7], and copper matrix [8-15]. Being one of the production methods using PM, Hot Pressing (HP) provides advantages

*) **Corresponding author:** ikirik@bingol.edu.tr

like full densification capability, short processing time, uniform dispersion of the reinforcing element, and shape production [16,17]. For bronze, two basic production methods are used; the first one is cast onto the steel and the other is powder metallurgy (PM) to produce a bimetal strip [18,19]. While conventional bronze contains nickel as an alloying element, copper is one of the basic components [20]. When nickel bronze is applied, refines the grain texture in the microstructure, enhances the mechanical properties and facilitates cold rolling. Furthermore, bronze composites with 5% nickel do not oxidize, do not change and have good resistance to rapid steam flows. Due to excellent wear resistance, microhardness and toughness, particle-reinforced MMCs are used for structural and high-temperature applications. Alumina and silicon carbide-based MMC do not lose their wear resistance and hardness [21-25]. Tin bronzes, Ni/Al bronzes and Cu alloys are the most commonly used bronzes. Tin bronzes are less frequently used compared to other kinds of bronze because of their high density and (consequently) high costs. These bronzes are used for bushings operating at low and high speed, worm screw, gear manufacturing, slipper, press bushing and slide bearings and they are used as gearbox replenishment pins in heavy vehicles that operate with high stroke [26-29]. Sn bronzes are the preferred copper alloys in many tribological applications due to their wear resistance and lubricating properties [30,31]. Ni/Al bronzes are accepted as perfect materials for applications requiring superior wear, high corrosion resistance, and high electrical/thermal conductivity. Ni has an attractive matrix due to its heat resistance. However, nickel catalyzes carbon crystallization when heated, resulting in degradation. Thus, the strength of Ni-matrix composites decreases sharply above 600°C [30]. As a result, it is reported that adding Ni to bronze improves good characteristics and SiC, B4C, WC, Al_2O_3, and TiC reinforcements improve mechanical properties of MMCs [32-43]. From this point of view, it has been observed that there are a limited number of studies on nickel-doped bronze and TiC-reinforced composites.

Therefore, the aim of this study is to add nickel, cobalt, and TiC to Cu/Sn bronze and to investigate how the TiC content affects the microstructure, thermal properties, microhardness, impact toughness, and wear behavior of the composites.

2. Materials and Experimental Procedures

In this study, Cu, Sn, and Co powders were commercially obtained from Nanokar, Ni and TiC powders from Alfa Aesar. Table I shows the size dimensions, purity and physical properties of the powders. TiC-reinforced Ni-Co Bronze matrix composites were produced with the hot press technique (Fig. 1). Before hot pressing (HP), the powders were prepared in groups at the rates (in Table II) and mixed in the powder mixing machine at 25 rpm 1/min in stainless steel cylindrical box with a steel ball for 30 min. The mixtures of the powders were poured into a graphite die (5 x 10 x 25 mm) and produced at 800^{o}C under 16 MPa load for 15 min in an Argon atmosphere. In order to determine microstructure, the samples were prepared according to standard metallographic procedure and etched with a chemical mixture (50 ml of nitric acid and 50 ml of glacial acetic acid). SEM, XRD, and EDS analysis were carried out for the detection status of phase contents and microstructure. Moreover, microhardness was applied on the polished surface with 1mm interval according to the indentation method with the load of 0.1 kgf. In order to determine the thermal transmissions, the samples were cut in the sizes of 1 x 3 x 6 mm from the Ni-Co bronze+XTiC composites using wire erosion method. Thermal Analysis of Ni-Co bronze+XTiC composites was performed using Perkin Elmer Phyris TG/DTA thermal analysis system at the heating rate of 20^{o}C 1/min in air atmosphere in the temperature range of 30^{o}C and 950^{o}C using a platinum crucible. Ni-Co bronze+XTiC composites were subjected to a wear test using the Turkyus Podwt pin-on disk device in accordance with the ASTM G99 standard. The wear test was conducted under loads of 5, 7.5 and 10N at the sliding speed of 31.41 m/s, trace diameter of 6 mm and sliding distances of 500 m.

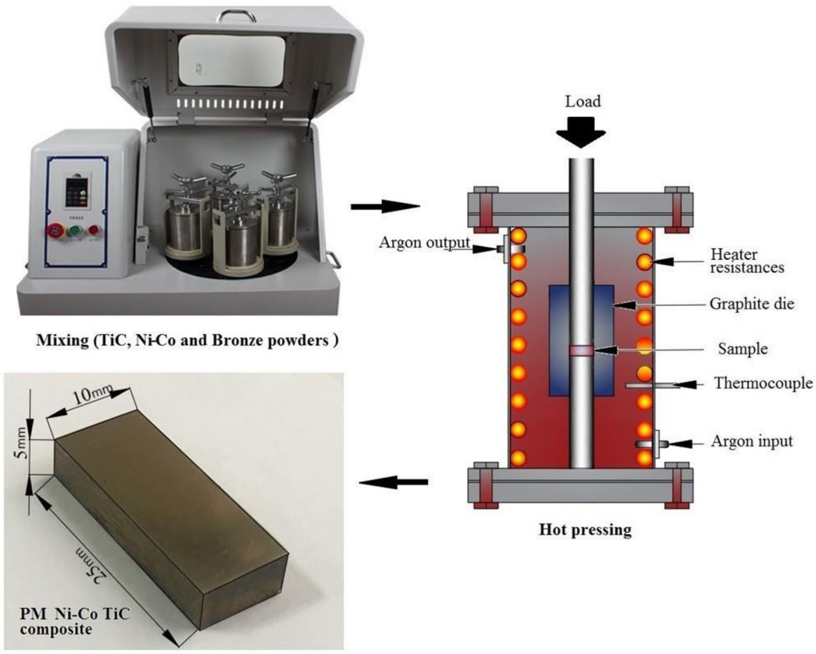

Fig. 1. The schematic illustration of PM Ni-Co-TiC composite production.

Tab. I The powder size distribution, dimensions, purity and physical properties of the powders.

Powder	Particle Size (µm)	Purity (wt.%)	Density ($g*cm^{-3}$)
Sn	45	>99.7	3.70 ± 0.30
Cu	45	>99.7	1,60 ± 0,10
Co	1.8 ± 0.2	99.7	8.86-8.90
Ni	44	99.8	0.60-0.75
TiC	45	99.5	4.5

Tab. II Quantities of powder used in the experiment (wt. %).

Material	TiC	Nickel (g)	Cobalt (g)	Bronze (CuSn90/10)(g)	Total (g)
Sample 1	0	5	5	15	25
Sample 2	3	5	5	15	25.75
Sample 3	7	5	5	15	26.75
Sample 4	10	5	5	15	27.5
Sample 5	15	5	5	15	28.75

3. Results and Discussion

3.1 Macro- and Microstructure examination

Fig. 2 shows the optic image of samples produced by adding 15 wt.% TiC. The image clearly shows that there were three different regions. The first of these regions was the matrix phase (A), the other was the reinforcement phase (B), and the third was the region where the reinforcement phase and the matrix phase were combined (C). The Ni-Co bronze+XTiC composites could be produced perfectly by using hot pressing method at 800^{o}C under 16 MPa for 15 minutes. When the microstructure images of Ni and Co-based TiC reinforced bronze were examined, it was observed that zones with different compositions formed in the microstructure at different rates of TiC. In the non-reinforced sample, only two zones formed, but from the picture and the EDS results obtained in the sample with TiC added, it was seen that there were three different regions between the matrix phase (white region) and TiC reinforcement, and Co, Ti and Cu elements were dominant in the interphase.

Figs 3a-e shows the SEM images of the samples S1, S2, S3, S4, and S5 manufactured with addition of Co using a hot pressing technique. Table III shows the EDS marks taken from these samples, respectively. The SEM microstructure image of Ni-Co bronze+XTiC composite showed that there was no cavity or defect in the interface of TiC reinforced Ni-Co bronze composites of all the samples. Fig. 3a shows preferably agglomerated zones with completely irregular and different sizes. However, the EDS results of different zones showed that when Co was added to the Ni-bronze, there were two regions that did not dissolve in each other and preferably unite in different ways. One of them was Ni-based (zone A) and the other was Co-based (zone B). Although these regions were seen as different formations, the boundaries of these two regions were clearly visible in the image (in Fig. 3a). When examining the SEM image of these TiC-reinforced composites (Fig. 3b-e), it was observed that the microstructure was composed of three structures; the preferably clumped plain light gray zones, regularly distributed zone containing TiC, and dark gray and sharp-edged grains representing TiC. Titanium carbides accumulated outside the bronze and Ni-containing regions. TiC and Co were both almost never seen within bronze grains. They were accumulated more in the boundaries of grains. When the SEM image of the sample containing 7 wt.% TiC was examined (Fig. 3d), it was observed that as TiC rate increased, Co-based zone was expanding and more regular. Despite higher density of the TiC grains, they still failed to enter the bronze phase (Fig. 3e). Buytoz et al., and Lee et al., [27,28] stated that the mechanical, thermal, and electrical properties of the composites were negatively affected by the randomly distributed reinforced particles. When the SEM image taken at high magnifications was examined (Fig. 3f), it was observed that the interphase bonding was good and it existed in a Co-rich region that held the matrix and reinforcement phases together.

Tab. III EDX results of Ni-Co bronze-XTiC composites (wt.%).

Elements	Marks										
	A	**B**	**C**	**D**	**E**	**F**	**G**	**H**	**I**	**J**	**K**
Ti	0.62	0.27	0.52	2.01	70.32	18.64	41.99	0.16	4.17	1	30.46
C	6.30	7.06	5.74	10.80	28.69	16.19	30.44	6.57	9.24	7.90	26.64
Ni	2.79	0	2.78	0.28	0.89	0	0	3.46	0.64	3.63	0
Co	0	71.05	0	71.98	0	51.49	0	0	75.79	0	26.58
Cu	83.28	19.48	84.24	13.63	0	11.14	23.92	83.68	9.16	81.63	14.42
Sn	7.01	2.13	6.62	1.30	0.10	1.74	3.65	6.13	1.01	5.78	1.96

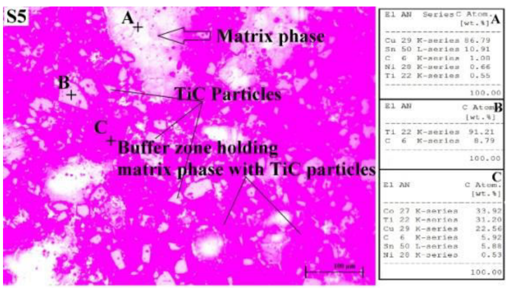

Fig. 2. Microstructure of Ni-Co bronze + wt.% 15 TiC composites.

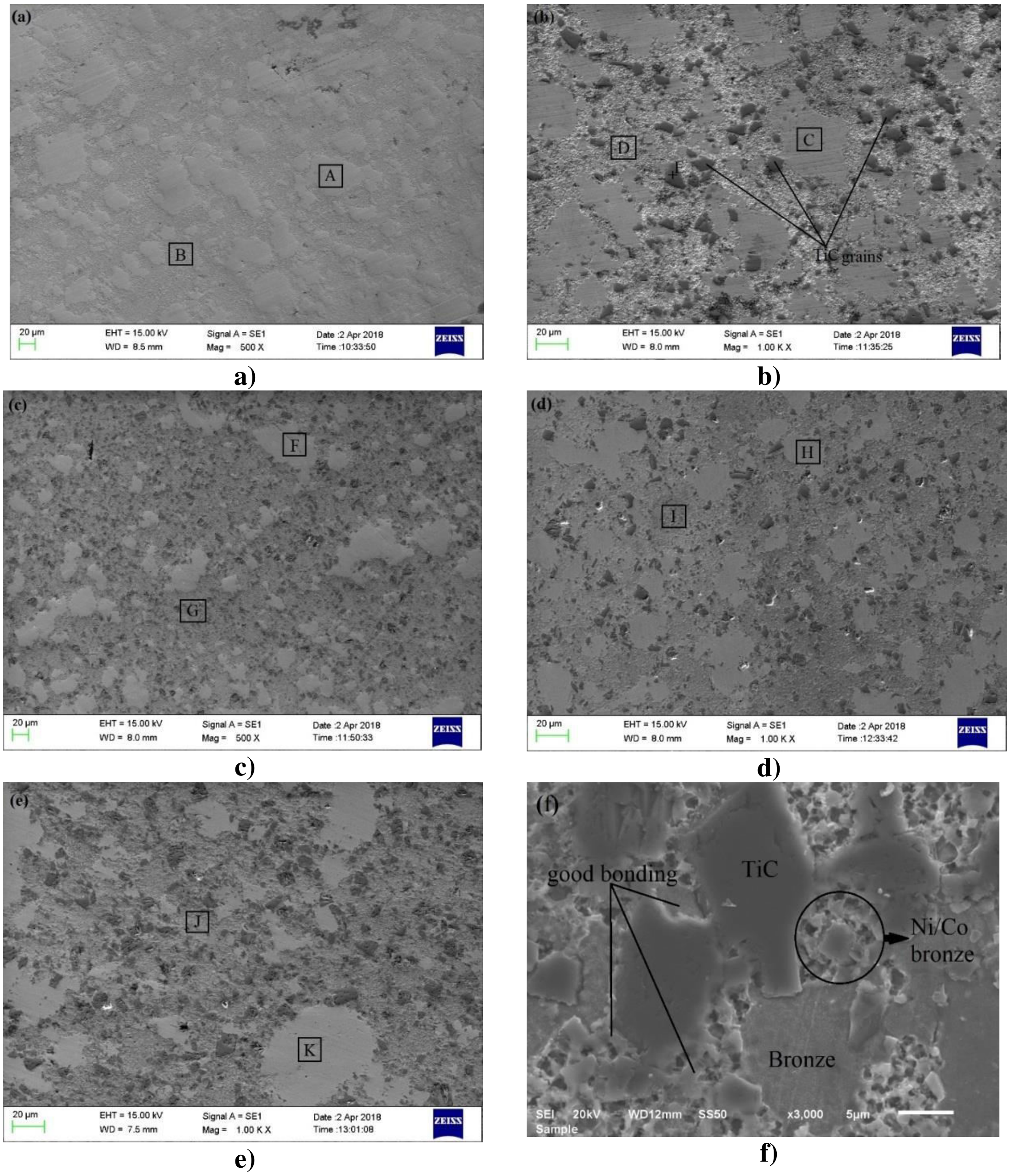

Fig. 3. SEM photographs of Ni-Co bronze+TiC_x composites: a) Ni-Co bronze no-reinforced, b) Ni-7Co bronze wt. % 3 TiC, c) Ni-Co bronze+wt.% 7 TiC, d) Ni-Co bronze+wt.% 10 TiC, e) Ni-Co bronze+15 wt.% 15 f) high magnification of S5 (e).

3.2 EDX and XRD analyses

EDX analyses taken from different zones are marked as A-K in Figs 3a-e. Based on the analyses, it is plausible to assert that Cu and Sn preferably agglomerated to form bronze (zones marked by A, C, F, H, and K). However, the Ni-Co bronze matrix, which was the main structure, existed in zones other than TiC particles (zones marked by B, D, G, I, and J). XRD analysis was performed for each composite to determine if there were phases supporting the formation of bonding between reinforcement (TiC) and matrix (Ni-Co bronze). As seen in Fig. 5, new phases such as NiTi, Ni3Ti, CuTi, CoNi, CuSn, and TiC were determined from XRD analysis. From these new phases and the locally collected elements that clumped in EDX analysis (see in Table III), there was a chemical bonding between the TiC (reinforcement) element and Ni-Co bronze (matrix). The presence of carbides and oxides is common in PM-prepared materials [39]. NiTi, Ni3Ti and CoNi phases were formed between titanium carbide and Nickel-based alloy. Based on XRD graphs of Ni-Co bronze+XTiC composites, no oxide was determined and when TiC rates increased, the peak of the graphs decreased.

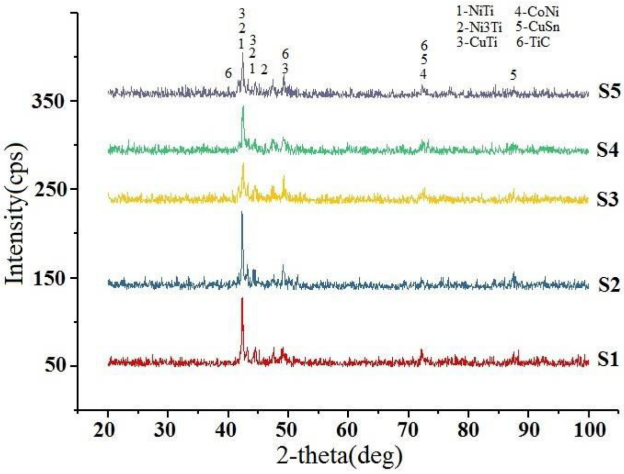

Fig. 4. XRD analysis of Ni-Co bronze+TiC_x composites.

3.3 Microhardness tests

Microhardness measurements were carried out at 1 mm intervals from a total of 17 points in the middle regions of the samples. Fig. 5 shows the results. The measured microhardness values varied between 180 and 540 Hv depending on TiC rates. Increasing TiC resulted in an increase in the microhardness value for all TiC-reinforced samples. As can be seen in this result, a significantly different trend was observed in the microhardness profiles. The hardness increased relatively with the reinforcement of TiC and this increase was almost twice in the TiC-reinforced samples compared to non-reinforced sample.

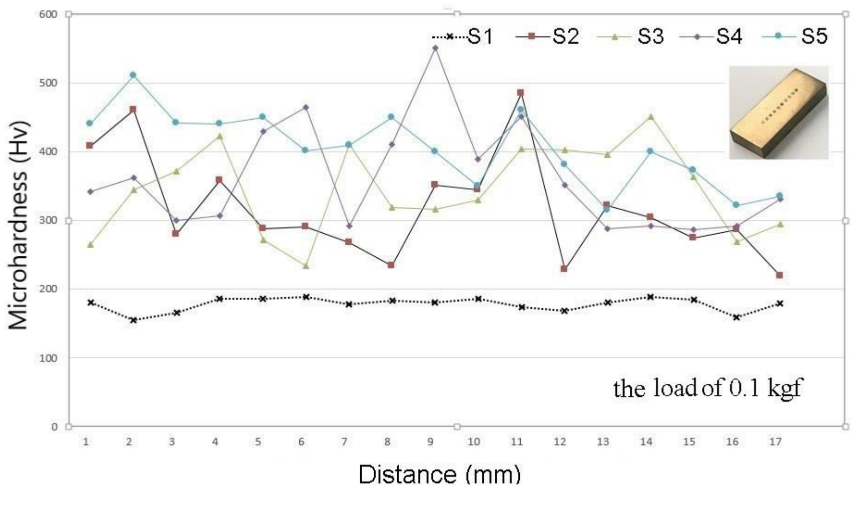

Fig. 5. Microhardness results of Ni-Co bronze+TiC (S1-S5).

3.4 Wear Behavior

The dry sliding wear test of Ni-Co bronze + XTiC composites was carried out using a stainless steel ball (Ø6 mm) in a pin-on-disc tester at room temperature. Fig. 6 shows the weight losses of composites from the wear tests. Increasing TiC rate also increased the hardness, which was effective on the decrease in the weight loss [20,21]. The wear resistance of the composites was contributed by adding TiC particles. The weight loss of the samples without TiC was 2-3 times higher than other samples with TiC. The weight loss decreased with increasing reinforcement rate under the loads of 5N, 7.5N, and 10N. The higher the load and/or sliding distance is caused the higher weight loss and wear rates [20-25]. Tyagi investigated the tribological behavior of Al/TiC composites in terms of the applied load and a constant sliding velocity. Moreover, the hard TiC particle blocked the metal flow from the surface of MMCs and improved their wear resistance [24,31]. When the content of TiC reinforcing phase in the composites reached 15 wt.%, the wear resistance of the composites decreased due to the separation of TiC particles from the surface depending on the effect of friction.

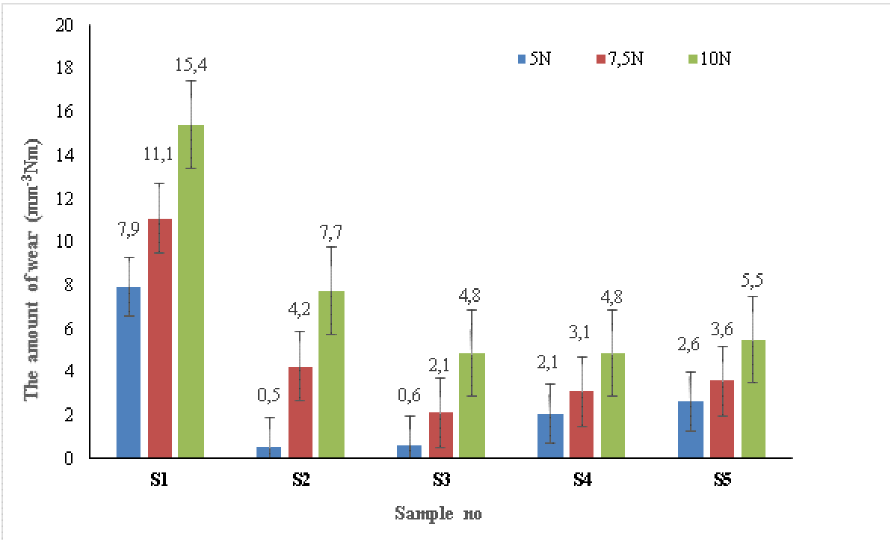

Fig. 6. The amount of mass loss depend of load Ni-Co-bronze + TiC_x composites.

Friction coefficient plots were determined during the wear tests depending on TiC rates and wear parameters. Fig. 7 shows the friction coefficients of the coating layers tested under 5N loads and different TiC rates. There were fluctuations in the friction coefficient depending on the sliding time. These fluctuations were big at the beginning. Over time, they increased (got even bigger) as the TiC rates increased (Fig. 8). When the abrasion coefficients were examined, the highest friction coefficient occurred in the sample containing no TiC and the friction coefficient decreased with the increasing TiC rate. The TiC reinforcement contributed to the reduction of the friction coefficient of Ni-Co bronze+XTiC composites. Even though the friction coefficient of the composites was lower than the friction coefficient of the material containing no TiC, the change in surface abrasion widely varied depending on the applied load. The EDS and XRD tests performed after wear revealed the friction coefficient decreased since the oxide formed on the surface and the carbides separated from the matrix during wear caused a lubricating effect on the surface. As a result, for increasing wear resistance in Ni-Co bronze, the TiC powder could be a reinforcement element candidate. Other studies [24,27,33] reported that the main reason for this behavior could be the presence of a lubricating layer forming on the surface, which did not lead to cohesive wear mechanism.

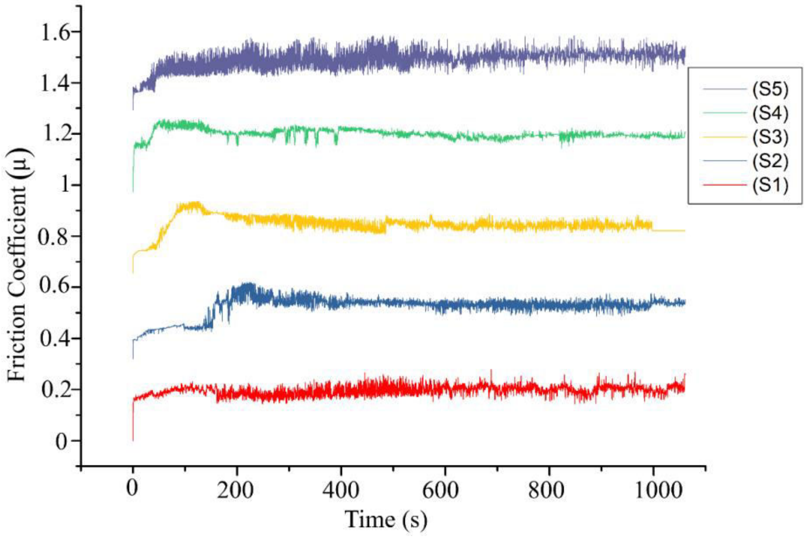

Fig. 7. Coefficient of friction depending on TiC rate composites.

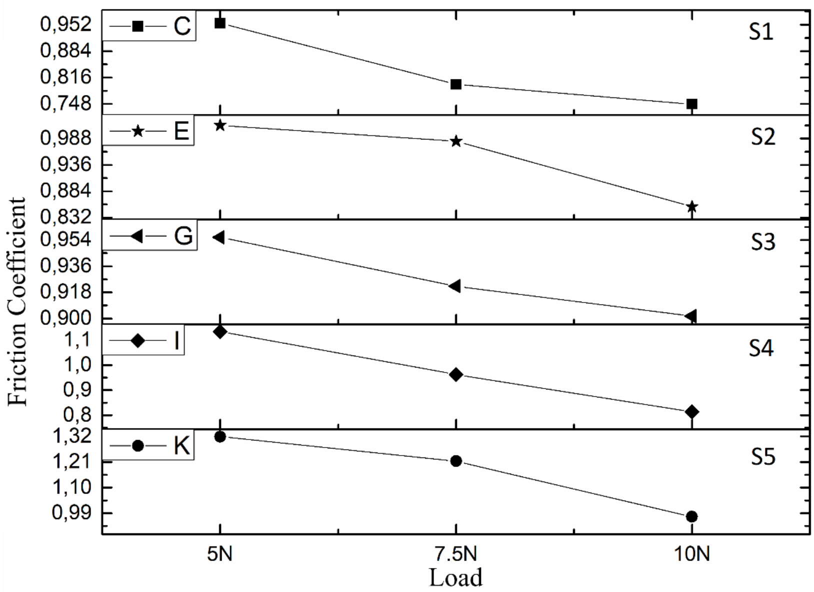

Fig. 8. Average coefficient of friction and mass loss for application load of 5N, 7.5N and 10N, respectivelly.

For further investigation of wear morphology, SEM analysis and EDX mapping taken from the surface of the samples were performed after the wear test (Fig. 9 a-e and Fig. 10a-e). The wear marks on the wear surface of the TiC-free sample were deeper and like a daisy. As the weight loss from the wear results was higher in this sample, the addition of TiC to Ni-Co bronze alloy will be an ideal reinforcement to gain wear resistance. In the image, the TiC grains broke from their places due to the effect of temperature and fracture that occur during wear and they were embedded in the bearings, where the ball passes, in the direction of successive rows. The reason of obtaining different wear rates and COF results was the carbide and oxide layers that formed due to the heat during wear between the steel ball and the composites. These layers prevent losses due to wear by making a lubricating effect. [4,20].

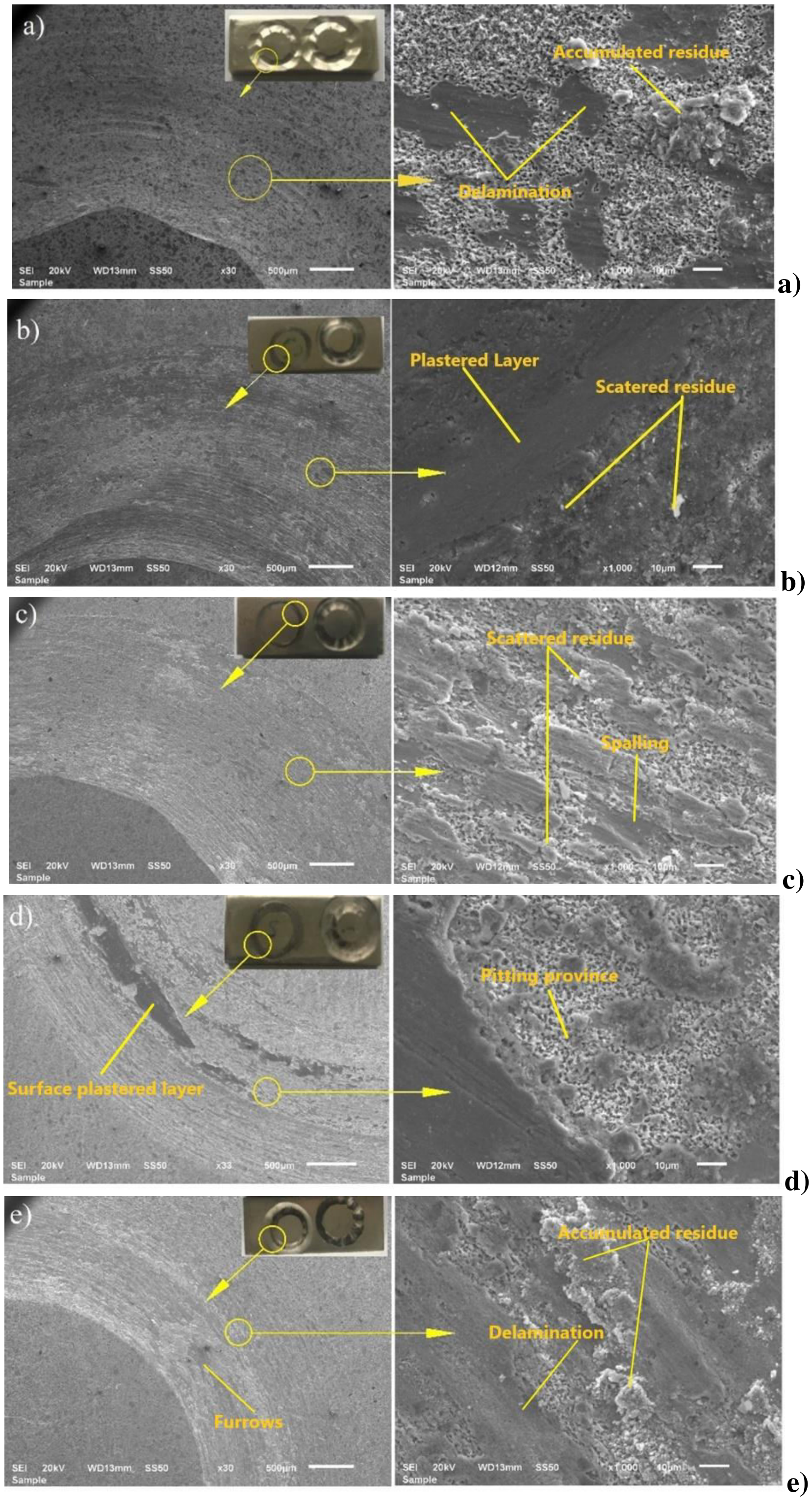

Fig. 9. SEM analysis of the worn surface of composites, a) Ni-Co bronze no-reinforced, b) Ni-Co bronze wt. % 3 TiC, c) Ni-Co bronze wt. % 7 TiC, d) Ni-Co bronze wt. % 10 TiC, e) Ni-Co bronze wt. % 15 TiC.

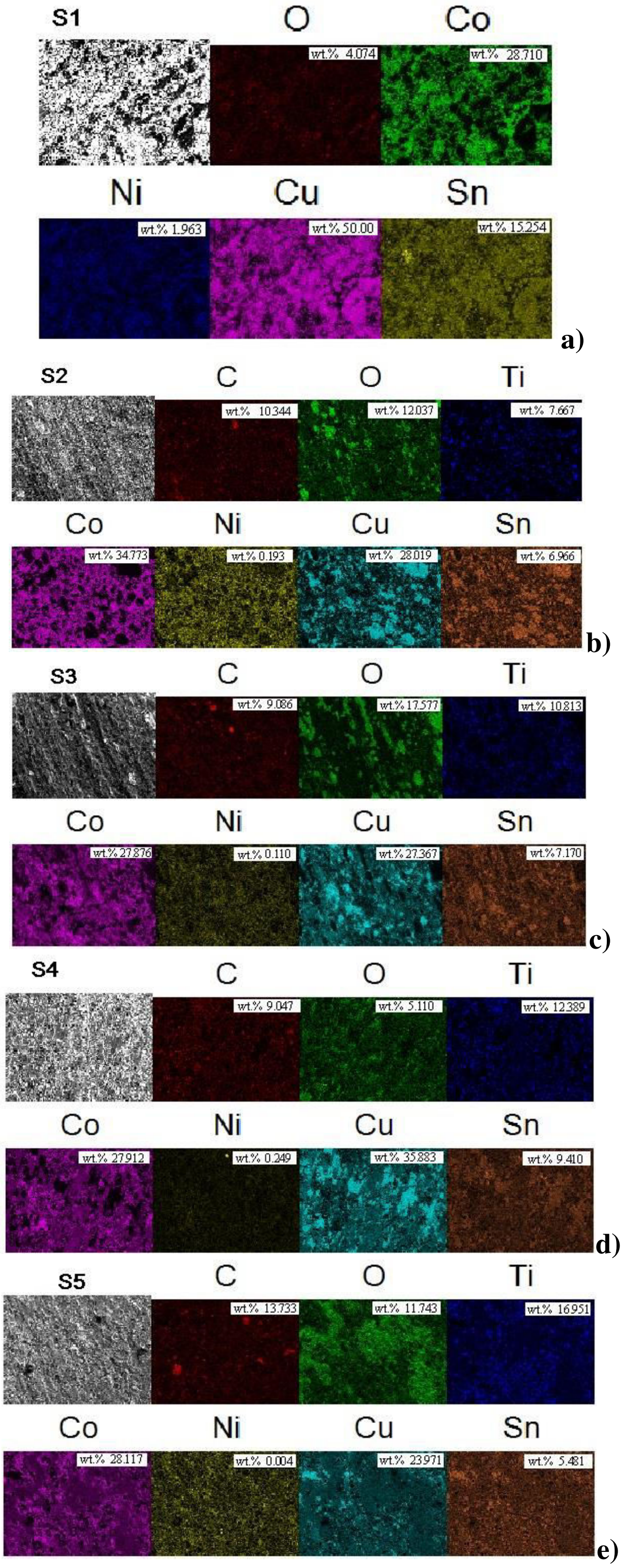

Fig. 10. EDX results of the worn surface of composites, a) Ni-Co bronze no-reinforced (S1), b) Ni-Co bronze wt. % 3 TiC (S2), c) Ni-Co bronze wt. % 7 TiC (S3), d) Ni-Co bronze wt. % 10 TiC (S4), e) Ni-Co bronze wt. % 15 TiC (S5).

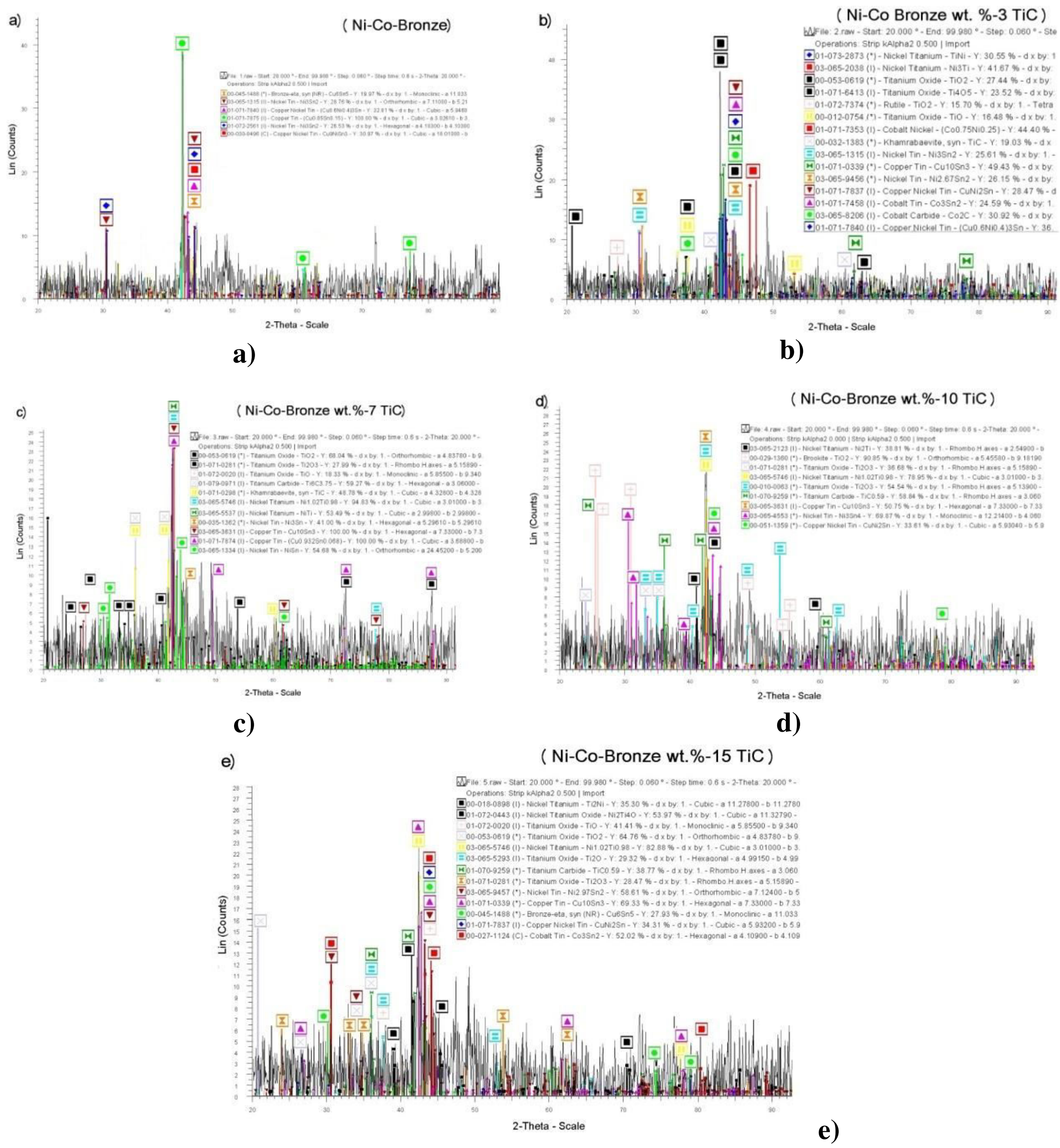

Fig. 11. XRD results of the worn surface of composites, a) Ni-Co bronze no-reinforced, b) Ni-Co bronze wt.% 3 TiC, c) Ni-Co bronze wt.% 7 TiC, d) Ni-Co bronze wt.% 10 TiC, e) Ni-Co bronze wt.% 15 TiC.

When the worn surfaces were examined, it was observed that the material losses on the surface of the Ni-Co-Bronze material were very severe. However, upon the addition of TiC to the Ni-Co bronze, not only the material peeling from surface layer decreased, but also the depth of the wear marks decreased. While the TiC rate increased from 3 wt. - % to 7 wt.%, the rate of wear decreased approximately three times, remained unchanged at 10 wt.- %, but increased slightly at 15 wt.- %. Many researchers have stated that this change is related to the degree of oxide film layer forming on the surface of the material [33-36]. XRD results taken from the worn surface are present in figures 11a-e, respectively. The presence of TiO, TiO_2, Ti_2O_3, Ti_4O_5, TiC and Ti_6C_4 compounds from the X-ray results taken from the surface supports the oxide and carbide layers forming in the surface layer of the TiC-reinforced samples. It was clearly seen that the oxide layer forming on the material surface not only acted as a lubricant, but also prevented material losses [36,37,42]. The addition of TiC to the

Ni-Co-Bronze alloy caused the material surface to heat up during friction and balanced the stresses that occurred during wear. The result evidently indicated that although the wear resistance increased with the increase of TiC rate (7-10 wt-%), the TiC rate had a negative effect at 15 wt.%. Residue accumulations and plastered residues occurred on the surface of the sample without addition of TiC. But, in the TiC-reinforced samples, scattered residue and plastered layer were more dominant. As a result, it was clear that the wear pattern was both oxidative and abrasive.

3.5 Impact properties

The effect of TiC contents on microstructure and charpy impact properties of Ni-Co bronze + TiC was investigated. For this purpose, the Charpy impact tests of the composites were carried out by using TERCO MT 3016 impact tester at the maximum energy of 150 Nm (Fig. 12). The tests were performed at room temperature regardless of the effect of temperature. Figure 13 shows that after the impact test, the charpy energy decreased with increasing TiC rate and the highest absorbed energy was obtained in the sample without TiC value (around 22J). As the TiC rate increased, the impact energy decreased sharply and then slightly less and lastly reached the minimum of 13 J when the TiC content was 15 wt.% (S5).

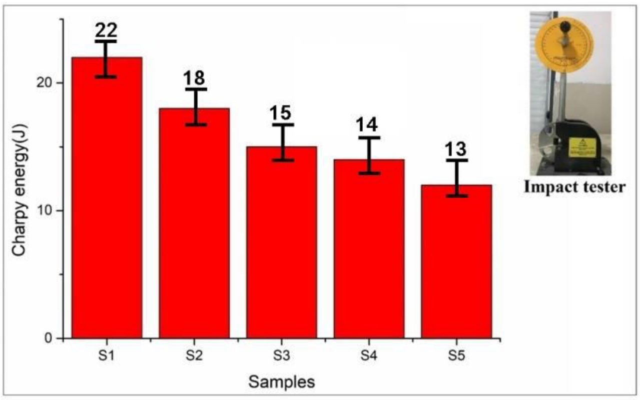

Fig. 12. Charpy impact test results of composites.

Fig. 13a-e shows the SEM images of fractured surfaces of the samples S1, S2, S3, S4, and S5, respectively. When the fractured surface images were examined, various voids and drop areas were observed in the non-reinforced sample, which were typical indicators of ductile fracture. The 3 wt.% TiC reinforced sample showed brittle fracture compared to non-reinforced sample (Fig. 13b). Although the fracture type of the samples S3, S4, and S5 was brittle, there is no ductile separation with bonding phase residues on the TiC grains, it looks more like decohesive separation. (Fig. 13c-e). It is plausible to assert that with the increasing rate of TiC, two phases (bronze and Ni-Co bronze+XTiC) agglomerated to a finer grain in the matrix.

3.6. Thermal properties

In this study, TG/DTA analyses were performed to determine the thermal properties of different TiC-reinforced composites. The measurements of all the samples were made at 30- 1000°C in an air atmosphere at a heating rate of 20°C min^{-1}. Then, TG/DTA curves were prepared using origin pro 8 program via the help of data obtained at different temperatures and given in Fig. 14a-b. Based on the TG analyses conducted to observe the changes in weights of the composites depending on time or temperature, the weight loss in Ni-Co bronze composites with TiC reinforcement was approximately 7% greater than the non-reinforced sample. When the TG curves were examined, the fluctuations were determined to be more in the non-reinforced sample, but the other samples exhibited a quieter pattern. Considering that the weight change occurs as a result of the breakage of physical or chemical bonds at high temperatures[27,41]. Moreover, it can be asserted that the bonding between TiC particles and matrix separated more easily at high temperatures.

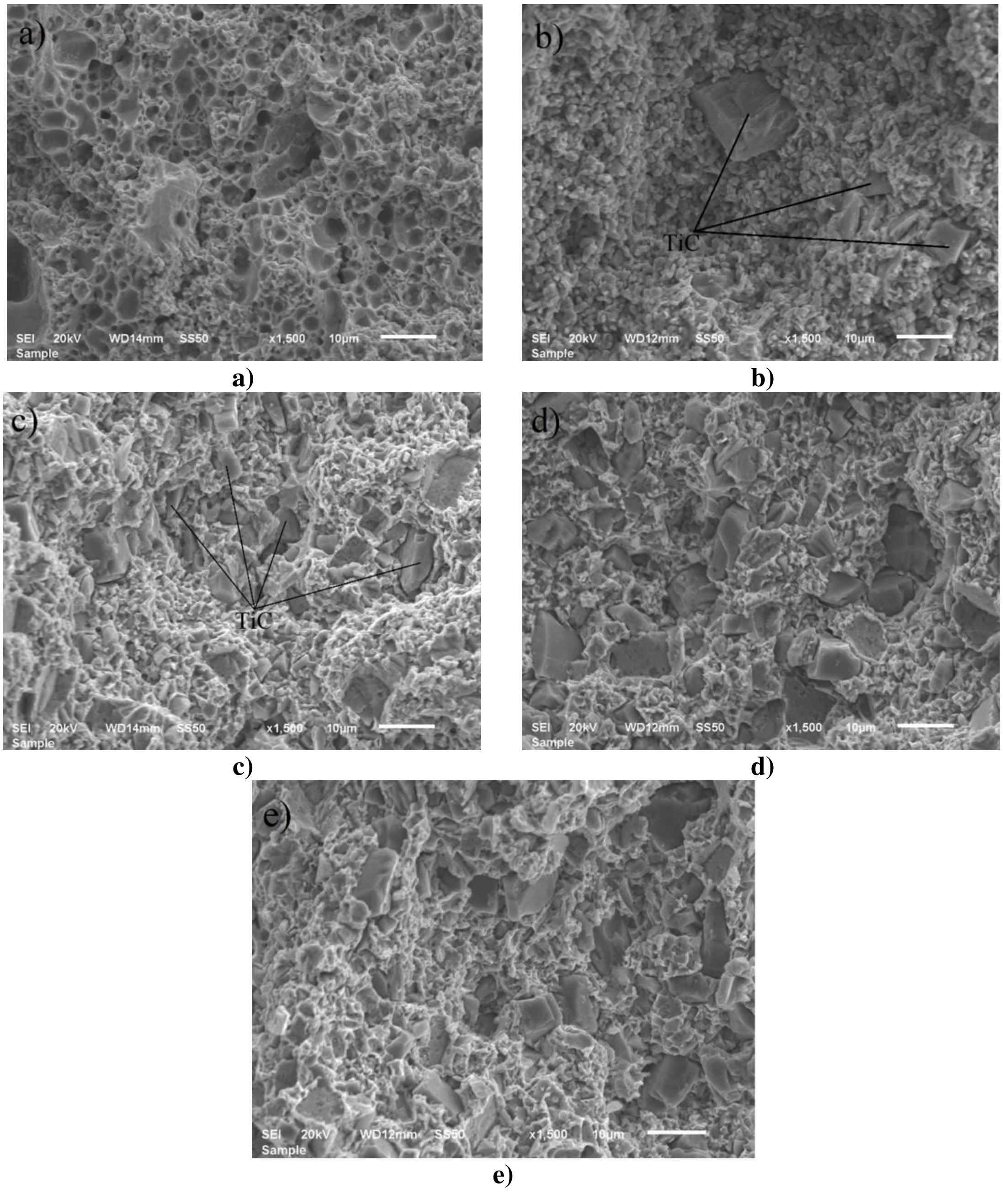

Fig. 13. SEM images of fracture surface morphologies of Ni-Co bronze with different TiC contents, a) S1, b) S2, c) S3, d) S4 and e) S5, respectively.

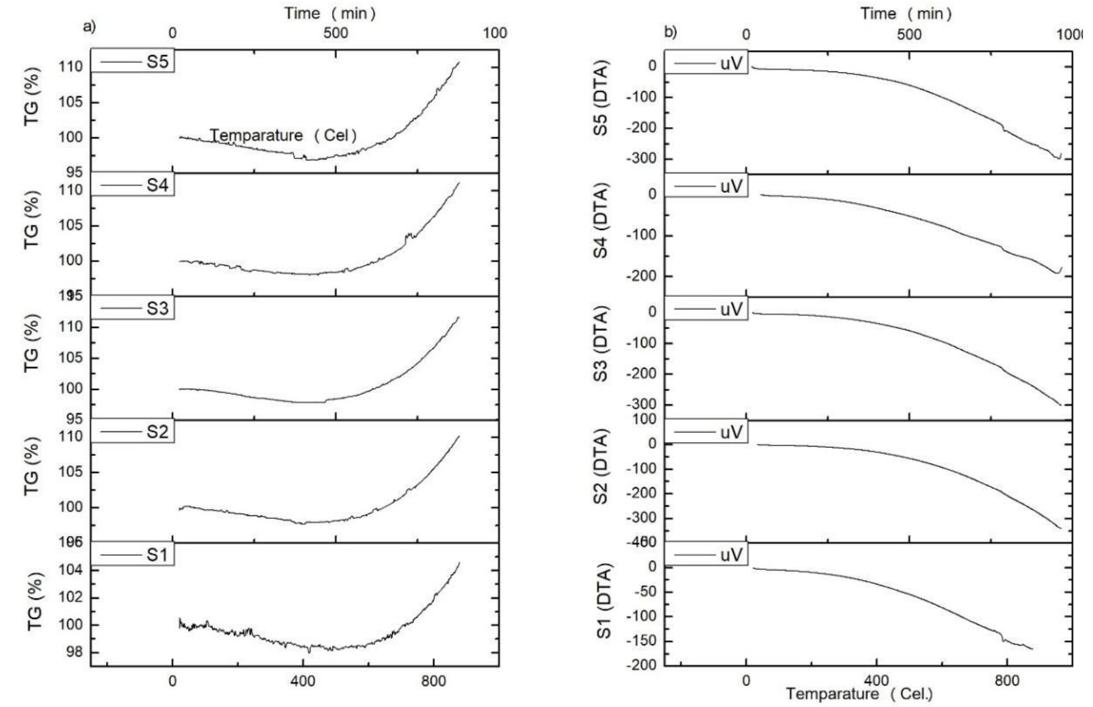

Fig. 14. a) TG curves and b) DTA curves of Ni-Co bronze + TiC_x composites.

4. Conclusion

In this study, Ni-Co bronze+XTiC with different TiC rates were produced by hot pressing method and following results were obtained.

1. From the microstructure examination of Ni-Co bronze + XTiC composite, there was no cavity and defect in the microstructure of composite.
2. In the SEM image of non-reinforced sample preferably agglomerated regions with completely irregular and different sizes were seen. Moreover, the EDS results from different regions showed that when Co was added to the Ni-bronze, there were two regions that did not dissolve in each other, and preferably unite in different ways. However, in the SEM image of TiC-added composites, the microstructure was composed of three different structures. First was the preferably clumped plain light gray areas, second was regularly distributed area containing TiC and third was dark gray and sharp-edged grains representing TiC.
3. From XRD analysis, new phases such as NiTi, Ni_3Ti, CuTi, CoNi, CuSn, and TiC were determined. Based on XRD graphs of Ni-Co bronze+XTiC composites, no oxide was determined.
4. These results showed that the hardness increased with the addition of TiC and this increase was almost twice the sample of TiC free.
5. The wear resistance of the composites was contributed by adding TiC particles. The weight loss of samples without TiC was 2-3 times higher than other samples with TiC. The wear pattern was both oxidative and abrasive. When TiC reinforcement exceeded 3 wt.%, less deep scratches and more plastered layers appeared on the surface of composites and the material degradation area gradually decreased.
6. The structural features which were listed above and the properties of Ni-Co bronze+XTiC composites such as micro hardness and wear resistance, were increased in a controlled manner but fracture toughness decreased.

5. References

1. M. Azizieh, D. Iranparast, M.A.G. Dezfuli, Z. Balak, H.S. Kim, Fabrication of Al/Al_2Cu in situ nanocomposite via friction stir processing, Trans. Nonferrous Met. Soc. China, , 27 (2017) 779-788.
2. P. Tallafuss, J. Johnston, Defects, causes and prevention controls in the continuous bronze/ steel bimetal strip sintering process, Eng. Failure Anal., 92 (2018) 32-43.
3. M. Barmouz, M.K.B. Givi, Fabrication of in situ Cu/SiC composites using multi-pass friction stir processing: evaluation of microstructural, porosity mechanical and electrical behavior, Compos. Part A-Appl. S., 42 (2011) 1445-1453.
4. P. Zhang, L. Ye, Y.W. Mai, G.F. Quan, W. Wei, Investigation on diffusion bonding characteristics of SiC particulate reinforced aluminium metal matrix composites (Al/SiCp-MMC), Compos. Part A., 30 (1999) 1415-1421.
5. Hascalik, N. Orhan, Effect of particle size on the friction welding of Al_2O_3 reinforced 6160 Al alloy composite and SAE 1020 steel, Mat. Design., 28 (2007) 313-317.
6. Kehler, R. Bode, H. Haddenhorst, Particle reinforced light metals, Partikelverstärkte Leichtmetalle Metall., 49 (1995) 191-195
7. Q. Han, K.C. Chan, Superplastic deformation mechanisms of particulate reinforced aluminium alloy matrix composites, Mater. Sci. Eng., 212 (1996) 256-264.
8. J. W. Kaczmar, Effect of production engineering parameters on structure and properties of Cu–W composite powders, Powder Metall., 32 (1989) 171-175.
9. N.C. Kathari, Sintering behaviour of copper containing titania, Modern Develop. Powder Metall., 16 (1984) 361-376.
10. U Upadhyaya, G.S. Upadhyaya, Sintering of copper-alumina composites through blending and mechanical alloying powder metallurgy routes, Mater. Design., 16 (1995) 41-45.
11. S. Chang, S. Lin, Fabrication of SiCw reinforced copper matrix composite by electroless copper plating, Scrip Mater., 35 (1996)225-231.
12. R. Ritasalo, X.W. Liua, O. Söderberg, A. Keski-Honkola, V. Pitkanen, S-P. Hannula, The microstructural effects on the mechanical and thermal properties of pulsed electric current sintered Cu-Al2O3 composites, Proc. Eng., 10 (2011) 124-129.
13. M. Barmouz, P. Asadi, M.K.B. Givi, M. Taherishargh, Investigation of mechanical properties of Cu/SiC composite fabricated by FSP: effect of SiC particles size and volume fraction, Mater. Sci. Eng. A., 528 (2011) 1740-1749.
14. J.J. Conway, Hot isostatic pressing of metal powders, Powder Metal Technol. Appl., (2004) 49-53.
15. E. Sap, Microstructural and mechanical properties of Cu-based Co-Mo-reinforced composites produced by the powder metallurgy method, J. Mat. Eng. Perform, (2020) 29.
16. K.G.K. Warrier, P.K. Rohatgi, Copper-titania electrical contacts, Powder Metall., 29 (1984) 65-69.
17. J.B. Fogagnolo, M.H. Robert, E.M. Ruız-Navas, J.M. Torralba, 6061 Al reinforced with zirconium diboride particles processed by conventional powder metallurgy and mechanical alloying, J. Mater. Sci., 39 (2004) 127-132.
18. Y. Ozcatalbas, E. Bahceci, M. Turker, Effect of cutting tool materials on surface roughness and cutting forces in machining of Al-Si3N4 composite produced by powder metallurgy, Mater. Sci. Forum., 534-536 (2007) 869-872.
19. M. A. Erden, A. M. Erer, Ç. Odabaşi, S. Gündüz, The Investigation of the Effect of Cu Addition on the Nb-V Microalloyed Steel Produced by Powder Metallurgy, Science of Sintering, 54 (2022) 153-167.
20. M.D. Huda, M.S.J. Hashmi, M.A. El-Baradie, MMCs: materials, manufacturing and mechanical properties, Key Eng. Mat., 104(10) (1995) 37-64.

21. O. Yılmaz, S. Buytoz, Abrasive wear of Al_2O_3-reinforced aluminium-based MMCs, Compo. Sci. and Technol., 61 (2001) 2381-2392.
22. S. Buytoz, M. Ulutan, M.M. Yildirim, Dry sliding wear behavior of TIG welding clad WC composite coating, Appl. Surf. Sci., 252 (2005) 1313-1323.
23. B.K. Prasad, Dry sliding wear response of some bearing alloys as influenced by the nature of micro constituents and sliding conditions, Met. Mater. Trans. A., 28 (1997) 809-815.
24. R. Tyagi, Synthesis and tribological characterization of in situ cast Al-TiC composites, Wear, 259 (2005) 569-576.
25. K.A. Smith, M.B. Zbib, D.F. Bahr, M.J.F. Guinel, Elastic behavior of a core-shell metal-carbon nanotube composite foam, MRS Commun., 4 (2014) 77-81.
26. M.Z. Huq, L.B. Celis, Reproducibility of friction and wear results is ball-on-disc unidirectional sliding tests of TiN-alumina pairings, Wear, 212 (1997) 151-159.
27. S. Buytoz, F. Dagdelen, S. Islak, M. Kok, D. Kir, E. Ercan, Effect of the TiC content on microstructure and thermal properties of Cu-TiC composites prepared by powder metallurgy, J. Therm. Anal. Calorim., 117 (2014) 1277-1283.
28. D.W. Lee, G.H. Ha, B.K. Kim, Synthesis of Cu-Al2O3 nano composite powder, Scrip Mater., 44 (2001) 2137-2140.
29. N.Y. Sari, M. Yilmaz, Improvement of wear resistance of wire drawing rolls with Cr–Ni-B-Si+WC thermal spraying powders, Surf. Coating. Technol., 202 (2008) 3136-3141.
30. D.Deborah, D.L.Chung, Metal-Matrix Composites, Elsevier BV., 2017
31. T. Yildiz, S. Aba, The effect of sintering temperature on wear resistance of alloys produced by using hot ısostatic pressing (HIP) method, J. Superhard Mater., 41 (2019) 157-168.
32. T.U. Kocak, H. Yanar, G. Purcek, F. Birol, Comparison of wear and friction properties of a nickel aluminum bronze (CuAl10Ni5Fe4) and Tın bronze (CuSn11), 2^{nd} Int. Iron and Steel Symp. (IISS'15) Karabük, Turkey, 1-3 April, 2014
33. S.C. Tjong, K.C. Lau, Tribological behavior of SiC particle-reinforced copper matrix composites, Material Letters, 2000, 43, p 274-280, doi.org/10.1016/S0167-577X(99)00273-6
34. A. Zhang, J. Han, B. Su, P. Li, j. Meng, Microstructure, mechanical properties and tribological performance of CoCrFeNi high entropy alloy matrix self-lubricating composite, Mater. Des., 114(2017) 253-263.
35. Y. Yu, F. He, Z. W. Liu, J. Yang, Effects of temperature and microstructure on the triblogical properties of CoCrFeNiNbx eutectic high entropy alloys, J. Alloys Compd., 775 (2019) 1376-1385.
36. J. Joseph, N. Haghdadi, K. Shamlaye, P. Hodgson, M. Barnett, D. Fabijanic, The sliding wear behavior of CoCrFeMnNi and AlxCoCrFeNi high entropy alloys at elevated temperatures, Wear, 428-429 (2019) 32-44.
37. M.L. Liang, C.L. Wang, C.J. Liang, Y.G. Xie, W.J. Liu, J.J. Yang, H. Tan, S.F. Zhou, Microstructure and sliding wear behavior of FeCoNiCr0.8Al0.2 high-entropy alloy for different durations, Int. J. of Refract. Metal. and Hard Mater., 103(2022) 105767.
38. T. Yildiz, N. Kati, A.K. Gür, The effect of sintering temperature on microstructure and mechanical properties of alloys produced by using hot isostatic pressing method. J.of Alloys and Comp., 737 (2018) 8-13.
39. M. Kılıç, E. Çetkin, I. Kırık, Z. Balalan, The production of TiC-reinforced nickel-bronze matrix composites by hot pressing method, 4th International Science Symposium, ISS2019 (September 4-6, 2019) ID : 2019.2A2PB.
40. O. Adam, V. Jan, Microstructure evolution of Cu-Fe-based immiscible alloys prepared by powder metallurgy, IOP Conf. Series: Materials Science and Engineering, 1178 (2021) 012001.

41. E. Sap, and M. Uzun, A study of the microstructure and properties of copper composites reinforced with Co-Ti, Metal Science and Heat Treatment, 63 (2022) 9-10.
42. Z. Özkan, H. Gökmeşe , U, Gökmen, Investigation of the Microstructure-Hardness and Wear Performances of Hybrid/Composite Materials Al_2O_3/SiC Particle Reinforced in AA 7075 Matrix, Science of Sintering, 54 (2022) 177-187.
43. M. Akkaş, F. R. A. A. Sudani, Effect of Hot Pressing and Reinforcement of TiC and WC on the Mechanical Properties and Microstructure of AlCuFeCrNi HEAs Alloy, Science of Sintering, (2021) 19-35.

Сажетак: *Побољшање микроструктурних, механичких и термичких својстава Ni-Co - бронза композита је кључно за различите примене. У овој студији, методом топлог пресовања произведено је пет Ni-Co-бронза (CuSn)+XTiC (0, 3, 7, 10, и 15 wt.%) композита. Истражен је утицај брзине ојачања TiC на сваку њихову микроструктуру, хабање, тврдоћу и термичка својства. У оквиру анализе микроструктуре коришћени су скенирајући електронски микроскоп (СЕМ), електронски дисперзивни спектрометар (ЕДС) и XRD анализа. Термичке анализе су извршене за одређивање термичких разлика између узорака. Поред тога, извршена су испитивања микротврдоће, удара и хабања да би се проценило механичко понашање Ni-Co бронза+XTiC композита. Експериментални резултати су показали да је удео TiC имао важан утицај на микроструктуру, отпорност на хабање и микротврдоћу Ni-Co бронзаног композита. Како се повећавала стопа ојачања TiC, тврдоћа Ni-Co бронза+XTiC композита је варирала између 180 HV и 450 HV. Сходно томе, анализа микроструктуре је открила да постоји озбиљна веза између ојачања и матрице. Отпорност на хабање је повећана са (7-10) теж. % TiC, али се смањила при високим уделима TiC. Јасно се видело да је образац хабања био и оксидативни и абразиван.*
Кључне речи*: Ni-Co бронза + XTiC композити, топло пресовање, термална анализа, жилавост, анализа истрошене површине.*